CRITICAL RAW MATERIALS ELIMINATION BY A TOP-DOWN APPROACH TO HYDROGEN AND ELECTRICITY GENERATION

Grant agreement no.: 721065

***Start date**: 01.01.2017 – **Duration**: 42 months*

***Project Coordinator**: CNRS*

DELIVERABLE REPORT

DELIVERABLE 3.4 – CRM-FREE METAL-N-C MATERIALS AS ORR CATALYSTS: SYNTHESIS, CHARACTERIZATION AND PERFORMANCE IN AEMFC & BMFC	
Due Date	29/02/2020 (M38)
Author(s)	Frédéric Jaouen, Pietro Giovanni Santori, Florian Speck, Serhiy Cherevko
Work Package	WP3: Catalyst synthesis and characterization
Work Package Leader	Tanja Kallio (AALTO)
Lead Beneficiary	CNRS
Date released by WP Leader	11/03/2020
Date released by Coordinator	12/03/2020

DISSEMINATION LEVEL		
PU	*Public*	***PU***
PP	*Restricted to other programme participants (including the Commission Services)*	
RE	*Restricted to a group specified by the consortium (including the Commission Services)*	
CO	*Confidential, only for members of the consortium (including the Commission Services)*	

NATURE OF THE DELIVERABLE		
R	*Report*	***R***
P	*Prototype*	
D	*Demonstrator*	
O	*Other*	

SUMMARY	
Keywords	oxygen reduction reaction, alkaline media, electrocatalyst, catalyst, critical raw material, iron, manganese
Full Abstract (Confidential)	The report presents the synthesis, activity and stability data for Fe-N-C and Fe-N-C/Mn-oxide composite electrocatalysts in alkaline electrolyte, measured with rotating ring disk electrode and scanning flow cell in liquid alkaline electrolyte first. Results obtained in AEMFC are then reported, including durability over 100 h at constant current density. The results show high activity at 0.9 V, high power performance in air/H_2 AEMFC and promising durability during AEMFC operation with Fe-N-C cathodes and PtRu/C anodes. The activity at 0.9 V in AEMFC is higher than that obtained with 0.4 mg_{Pt} cm^{-2} state-of-art cathodes, while slightly lower performance is seen at high current densities, assigned to lower accessibility of FeN_x sites due to the microporous nature of the carbon matrix in Fe-N-C and also due to the lower site density in Fe-N-C vs. Pt/C. The composite Mn_2O_3/Fe-N-C showed similar high initial performance than Fe-N-C, and showed lower production of peroxide in rotating ring disk electrode setup.
Publishable Abstract (If different from above)	

CONTENTS

INTRODUCTION

The purpose of D3.4 is to demonstrate the preparation of optimized Fe-N-C catalysts and to characterize them for Oxygen reduction reaction (ORR) in alkaline medium first, and then in AEMFC and also in BMFC if a bipolar membrane (BM) with sufficient through-plane conductivity is available at M38 (due date of this deliverable). The goal was to demonstrate a promising path for replacing platinum by cathode catalysts based on Earth-abundant elements in AEMFC and/or BMFC, with no or small performance drop when replacing Pt by non-PGM cathodes.

This report presents the synthesis of optimized Fe-N-C catalysts, their structural characterization, their electrochemical characterization in alkaline electrolyte (activity, selectivity, stability) and then their evaluation at the cathode of AEMFCs. Due to higher through-plane resistance of bipolar membrane than desired for high power density AEMFC at M38 and issues associated with the preparation of BM with H^+ and OH^- form on each side, testing of BMFC with Fe-N-C cathodes has not yet been performed. The promising results obtained with AEMFC with Fe-N-C cathodes and composite Mn-oxide/Fe-N-C cathodes however show that such cathodes would also be suitable for BMFC if a proper BM and MEA preparation for BMFC is available in the near future.

1. PROTOCOLS FOR THE ELECTROCHEMICAL MEASUREMENTS

1.1 EXPERIMENTAL CONDITIONS AND PROTOCOL FOR ORR ACTIVITY MEASUREMENT IN RDE

The electrochemical experiments were performed with a Biologic SP-300 potentiostat. A three-electrode cell configuration was used for all RDE/RRDE experiments using 0.1 M KOH as electrolyte solution, a reversible hydrogen electrode as a reference and a graphite plate as counter electrode. As working electrode, the catalyst ink was deposited in a glassy carbon. The catalyst-ink was prepared with 5 mg of Fe-N-C catalyst in 54 µL of ionomer (Nafion, 5% solution in lower alcohols), 744 µL of ethanol and 92 µL of ultrapure water. The ink was ultrasonicated one hour and the required aliquot was then deposited with a pipet on the glassy carbon, so that a catalyst loading of 0.2 $mg \cdot cm^{-2}$ is reached. Once the electrode was completely dry, a drop of water was deposited on it to minimise the entrapment of air bubbles during the immersion of the shaft and rotating disk electrode (RDE) tip in the electrolyte. N_2 was bubbled in the electrolyte for 30 minute, then the cyclic voltammogram in N_2-saturated electrolyte was recorded by scanning the potential at 10 $mV \cdot s^{-1}$ between 0.0 and 1.0 V vs. RHE for a few cycles, until reproducible scans were recorded. The electrolyte was then saturated with O_2 for 30 min, and the polarization measurements from which ORR activity is directly extracted were recorded at a low scan rate of 1 $mV \cdot s^{-1}$ in the potential range 0.0-1.1 V vs RHE, and at 1600 rpm rotation rate. It was verified that the scan rate of 1 $mV \cdot s^{-1}$ is low enough that capacitive current can be neglected for the investigated catalysts.

1.2 EXPERIMENTAL CONDITIONS AND PROTOCOL FOR ORR STABILITY MEASUREMENT IN RDE

Accelerated stability tests (AST) were performed by comparison between the initial polarization curve (following the procedure described above) and the polarization curve obtained with the same electrode after 5000 potential cycles between 0.6 and 1.0 V *vs*. RHE. The 5000 cycles were applied either in N_2-saturated or O_2-saturated 0.1 M KOH electrolyte (indicated in figure captions), at a scan rate of 100 $mV \cdot s^{-1}$ and without any rotation (AST protocols No. 1 and 2, as defined in Deliverable 2.1, "Definition of Test Protocols" of the project CREATE). For the final polarisation curve, a fresh electrolyte was used, and the same conditions as used for recording the initial polarisation curve were applied.

1.3 EXPERIMENTAL CONDITIONS AND PROTOCOL FOR STABILITY MEASUREMENT IN SCANNING FLOW CELL

The leaching of Fe during short electrochemical cycling, performed either before or after the AST, was investigated in an on-line electrochemical scanning flow cell (SFC) directly connected to an inductively-coupled plasma mass spectrometer (ICP–MS), previously developed by the Jülich partner. It is however impossible to continuously measure Fe leaching over the length of the AST, due to drift of the ICP-MS with time and need for constant recalibration. The SFC consists of a three-electrode setup using a Ag/AgCl (Metrohm, 3 M KCl) leaking reference electrode, a graphite rod counter electrode and a GC RDE as a working electrode, on which the catalyst is drop cast. A positioning stage (Physik Instrumente, M-403.6 DG) is used to approach individual catalyst spots on the working electrode. Stability measurements are

conducted in alkaline (99.99%, Suprapur®, NaOH, 0.05 mol·L^{-1}) electrolyte. The catalyst ink is prepared from the Fe-N-C catalyst, Nafion® (5% perfluorinated resin solution) and water, with a mass ratio of catalyst/dry-ionomer of 4 and a catalyst concentration of 3.3 g·L^{-1} in the liquid ink. An aliquot of 2.75 µL is deposited on the GC, resulting in a catalyst loading of 400 µg·cm^{-2}. Such a high loading is necessary to reach a sufficient signal-to-noise ratio. More details can be found in Ref. [1].

1.4 Membrane-electrode-assembly preparation and AEMFC test conditions

The anode catalyst was prepared by mixing 40wt%Pt-20wt%Ru/C (Johnson Matthey) with Vulcan carbon black, to reach a total Pt+Ru content of 40 wt% on carbon. The cathode catalyst was Fe-N-C, Mn_2O_3/FeNC, or Pt/C. The catalytic inks were prepared by grinding the catalyst (anode or cathode catalyst) and anion exchange ionomer (AEI) with water and propanol. The AEI content was 40 wt % with respect to the carbon contained in the anode, and 20 wt % with respect to carbon for $Fe_{0.5}$-NH_3 or Mn_2O_3/ $Fe_{0.5}$-NH_3 composites. The dispersion was then sonicated for 1 h and then sprayed on a gas diffusion layer (Toray 60, with 5 wt % PTFE wet-proofing). These ink preparation and electrode preparation methods have been recently developped by the group of William Mustain, at University of South Carolina (USA), and the AEMFC testing performed in collaboration with Mustain's group in order to test the Fe-N-C catalysts issued from CREATE in the best conditions. [4] The obtained gas diffusion electrodes and AEM were then soaked for 20 min in 1 M KOH, and this was repeated two times. The MEA was then assembled in the single-cell fuel cell hardware using Teflon gaskets, with gasket thickness chosen to reach 25% compression. The AEMFC was operated using a Scribner 850e Fuel cell test system, flowing H_2/O_2 at 1.0 L min^{-1} with a cell temperature of 65°C. The corresponding dew points were optimized for each MEA, but typically were 60°C at the cathode and 55°C at the anode. The break-in was performed in potentiostatic mode at 0.5 V.[4] All AEMFC experiments have been carried out using a loading of 0.6 mg_{Pt+Ru} cm^{-2} at the anode. The polarisation curves were recorded by scanning the cell voltage from OCV to 0.1 V at a scan rate of 10 mV s^{-1}.

1.5 Synthesis of ORR Catalysts

Fe-N-C catalysts: the Fe-N-C catalysts were obtained starting from a Zn-based zeolitic imidazolate framework (ZIF-8, Basolite® Z1200, from BASF), 1,10-phenanthroline (phen) and iron acetate. The powder precursors of ZIF-8, phen and ferrous acetate were mixed with low energy ball milling, resulting in a homogeneous catalyst precursor containing 0.5 wt% Fe before pyrolysis. This catalyst precursor was then pyrolyzed in argon at 1050°C for 1 hour (labelled $Fe_{0.5}$ -Ar), then pyrolyzed in NH_3 at 950°C for 5 min (labelled $Fe_{0.5}$-NH_3). More details can be found in Ref. [1].

Composite Mn-oxide/Fe-N-C: To functionalize Fe-N-C with a co-catalyst that can further scavenge hydrogen peroxide during AEMFC operation, various Mn-oxides were screened for their ability to electro-reduce HO_2^-. The Mn-oxide with best combination of peroxide reduction activity and stability was selected (Mn_2O_3), and then physically mixed with $Fe_{0.5}$-NH_3 in a mass ratio 20/80 ratio in order to prepare the composite Mn_2O_3/$Fe_{0.5}$-NH_3. For preparing α–Mn_2O_3, γ-MnOOH was prepared in a first step, and then calcined at 550°C for 12 h. For the first step, γ-MnOOH was synthesized dissolving $Mn(CH_3COO)_2{\cdot}4H_2O$ and $KMnO_4$ in deionized water, the solution refluxed for 12 h and then washed with water and dried.

2. STRUCTURAL CHARACTERIZATION OF Fe-N-C AND Mn_2O_3

2.1 STRUCTURAL CHARACTERIZATION OF Fe-N-C CATALYSTS

The pristine Fe-N-C catalysts were characterized with ^{57}Fe Mössbauer spectroscopy at room temperature. To this end, ^{57}Fe-enriched catalysts are used, prepared identically as the ones otherwise investigated in this study, except for the use of ^{57}Fe acetate during their synthesis. The pristine catalysts were also characterized with X-ray absorption spectroscopy (XAS) in *ex situ* conditions. The spectra were collected in fluorescence mode at SAMBA beamline at room temperature using a double crystal Si 220 monochromator.

The *ex situ* ^{57}Fe Mössbauer spectra could not reveal any significant difference between the two catalysts (Figure 1a-b). They were fitted with two doublets D1 and D2, each one having similar Mössbauer parameters for both catalysts and being present in similar ratio. These doublets are assigned to atomically-dispersed FeN_x moieties.[2-3] Similar Mössbauer spectra imply that the local Fe coordination and site geometry are similar in both catalysts. Further identification of the active-site structure was performed using *ex situ* XAS. Figure 1c shows the *ex situ* X-ray absorption near-edge structure (XANES) spectra of $Fe_{0.5}$-NH_3 (circle symbols) and $Fe_{0.5}$-Ar (solid curve), that are characteristic for Fe-N-C catalysts free or quasi-free of metallic particles.[2] The absence of a strong signal at *ca* 2.2 Å (Fe-Fe bond distance in metallic and metal-nitride particles, uncorrected for phase shift) in the FT-EXAFS spectra of both $Fe_{0.5}$-Ar and $Fe_{0.5}$-NH_3 indicates that both catalysts are free or quasi-free of Fe-based particles (Figure 1d). The white line intensity in the XANES spectra is slightly stronger for $Fe_{0.5}$-Ar than $Fe_{0.5}$-NH_3. This may be interpreted as a higher coordination number in the first coordination sphere surrounding Fe (either N, C or O atoms). This hypothesis is supported by the stronger signal of the first peak (at *ca* 1.4 Å) in the Fourier transforms (FT) of the extended X-ray absorption fine structure (EXAFS) spectra for $Fe_{0.5}$-Ar *vs.* $Fe_{0.5}$-NH_3 (Figure 1d). Such changes may be assigned to a stronger FeN_4-O_2 interaction *ex situ* for $Fe_{0.5}$-Ar, possibly due to a higher average oxidation state of Fe in $Fe_{0.5}$-Ar *vs.* $Fe_{0.5}$-NH_3. In the latter, a lower oxidation state of Fe may be expected due to the presence of Lewis-base (highly basic) nitrogen groups.

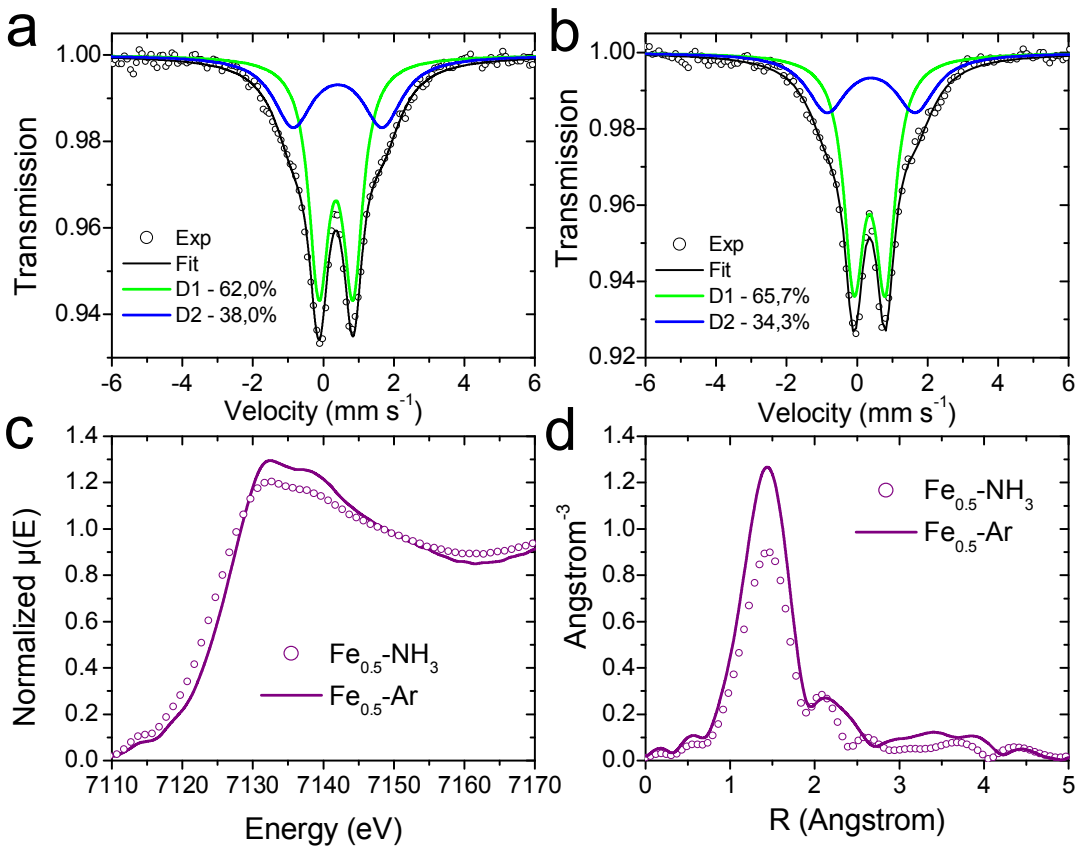

Figure 1. Ex situ spectroscopic characterization of $Fe_{0.5}$-NH_3 and $Fe_{0.5}$-Ar. ^{57}Fe Mössbauer spectroscopy (top) for a) $Fe_{0.5}$-Ar and b) $Fe_{0.5}$-NH_3. XAS characterisation at the Fe K-edge (bottom) by c) XANES and d) EXAFS. The spectra were recorded in air at room temperature. The distance in the FT-EXAFS spectra is not corrected for phase-shift.

2.2 Structural characterization of Mn_2O_3

SEM images of α-Mn_2O_3 are shown in Figure 2, with rather large particles of ca 100 nm. The measured BET area was only 14 $m^2\ g^{-1}$, and a rough estimation of expected BET area for 100 nm particle size of α-Mn_2O_3 shows that the SEM and BET area information are congruent, indicating the absence or low amount of intra-particle pores. Despite its low BET area, the Mn_2O_3 phase was shown to be as active, or even more active, towards ORR and HO_2^- reduction than other Mn-oxide polymorphs with higher BET areas, and was therefore selected to prepare composites with Fe-N-C.

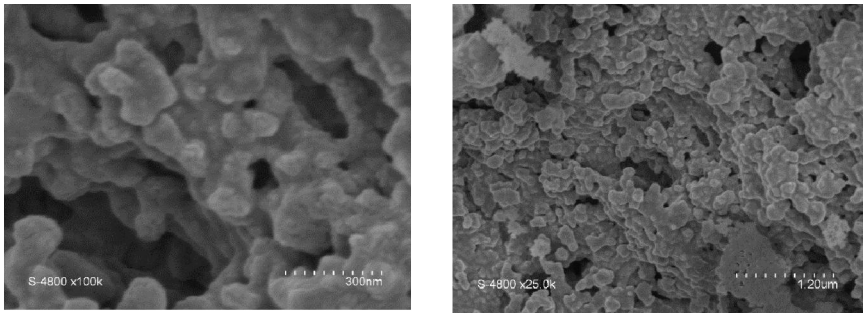

Figure 2. SEM images of Mn_2O_3 in two different magnifications

3. STABILITY AND ACTIVITY OF FE-N-C AND Mn_2O_3/FE-N-C CATALYST S IN LIQUID ELECTROLYTE

3.1 ROTATING DISK ELECTRODE MEASUREMENTS

The stability of the $Fe_{0.5}$-Ar and $Fe_{0.5}$-NH_3 catalysts was studied in alkaline electrolyte. Starting with $Fe_{0.5}$-Ar, the activity increased from 0.07 to 0.11 mA cm^{-2} at 0.9 V vs. RHE after 5000 load-cycles in N_2-saturated solution between 0.6 and 1.0 V vs. RHE (Fig. 3a-b). Similarly, also $Fe_{0.5}$-NH_3 shows high stability in alkaline electrolyte, with very slight decay in activity at 0.9 V *vs.* RHE (from 0.92 to 0.83 mA·cm^{-2}, Fig. 3c-d). Since the AST was performed in N_2-saturated electrolyte, no ORR occurred and we can exclude a degradation or deactivation due to hydrogen peroxide or reactive oxygen species formed from peroxide and FeN_x sites. In those conditions, both catalysts were quite stable, but $Fe_{0.5}$-NH_3 catalyst was much more active than $Fe_{0.5}$-Ar, assigned to the increased basicity of the surface due to the ammonia pyrolysis and also, as a secondary effect, due to increased specific surface area (ca 1000 vs. 500-550 m^2 g^{-1}).

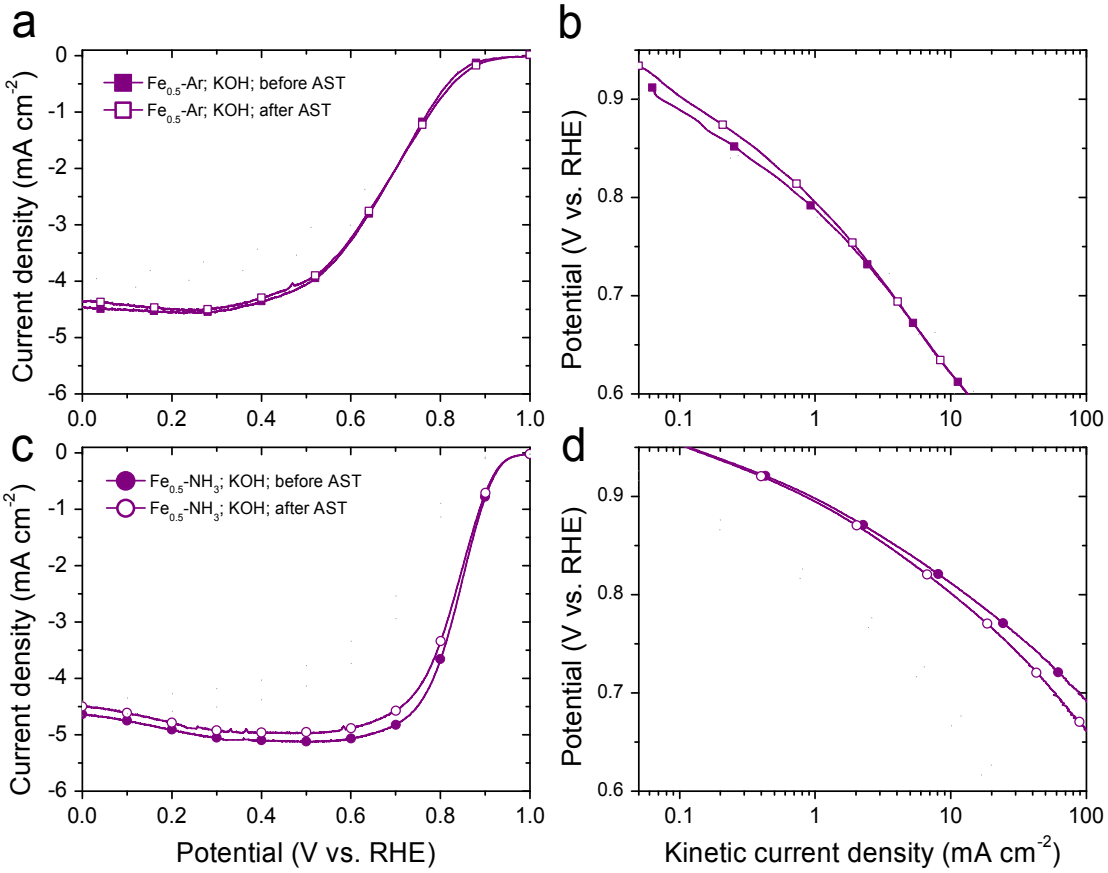

Figure 3. RDE determination of the ORR activity of $Fe_{0.5}$-Ar (a, b) and $Fe_{0.5}$-NH_3 (c, d) in alkaline electrolyte before (filled symbols) and after (empty symbols) the load-cycling AST. Polarisation curves were measured in O_2-saturated electrolyte at a scan rate of 1 mV s^{-1}, a rotation rate of 1600 rpm and a catalyst loading of 200 µg·cm^{-2}. The AST has been conducted in N_2-saturated electrolyte, in a potential range of 0.6-1.0 V vs RHE, with a scan rate of 100 mV s^{-1} for 5000 cycles. The semi-logarithmic Tafel plots on the left handside have been obtained from the polarisation curve by applying the Koutecky-Levich equation.

Figure 4 shows the higher activity toward HO_2^- electroreduction for the composite 20%-Mn_2O_3/$Fe_{0.5}$-NH_3 compared to $Fe_{0.5}$-NH_3 alone, visible from the much higher absolute value of current density at low potential. In the case of $Fe_{0.5}$-NH_3, the current density is lower than expected for 2-electron reduction of peroxide to water, due to site blocking effect of peroxide on FeN_x sites. With the addition of Mn_2O_3, this limiting step is not seen and the plateau of current density is close to that expected for two-electron reduction of HO_2^- in the rotating condition and peroxide concentration employed here. The composite 20%-Mn_2O_3/$Fe_{0.5}$-NH_3 is therefore promising for the reduction of peroxide production in operation in AEMFC.

The ORR activity and stability of the composite was also assessed (Figure 5), giving good results, with only a lower initial ORR activity of ca 20% for Mn_2O_3/$Fe_{0.5}$-NH_3 compared to $Fe_{0.5}$-NH_3, fully proportional to the dilution effect of FeNC by Mn-oxide (20 % Mn-oxide on Fe-N-C), logical since the total mass of FeNC + Mn_2O_3 was kept constant in the RDE measurements. The stability to 5,000 load cycles in O_2-saturated electrolyte leads to negligible ORR activity loss at 0.9 V, and slightly decreased diffusion-limited current density, which could be due to a change in the selectivity or change in mass-transport characteristics of the layer (Figure 5).

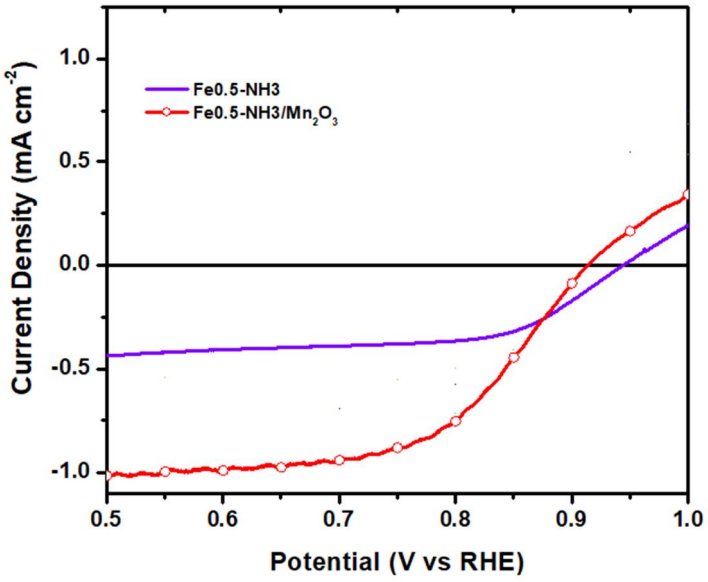

Figure 4. Activity for hydrogen peroxide electro-reduction of the 20%-Mn_2O_3/$Fe_{0.5}$-NH_3 composite and comparison to $Fe_{0.5}$-NH_3. The electrolyte is 2 mM H_2O_2 in a N_2-saturated 0.1 M KOH electrolyte. The polarisation curves are measured at 1 mV s^{-1} and 1600 rpm of rotation

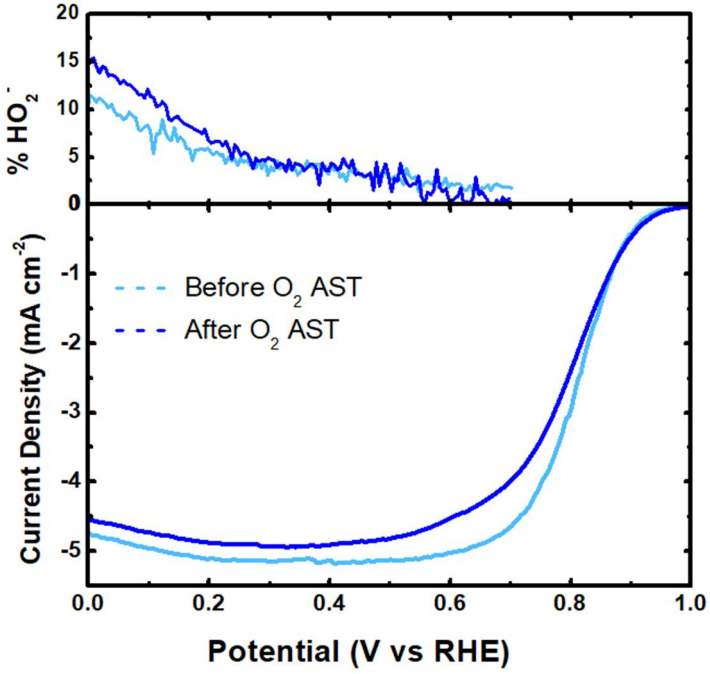

Figure 5. Activity for ORR of the 20%-Mn_2O_3/$Fe_{0.5}$-NH_3 composite. The polarization curves are taken at 1 mV/s in oxygen-saturated electrolyte, with a rotation rate of 1600 rpm, both before and after the load-cycle stress test. The electrolyte is 0.1 M KOH. The AST was 5,000 cycles between 0.6-1.0 V in O_2 saturated electrolyte.

3.2 SCANNING FLOW CELL MEASUREMENT OF METAL LEACHING RATES

To investigate the demetallation of iron *in situ*, we conducted SFC-ICP–MS measurements. Figure 6 summarizes the *operando* Fe leaching measurements on the two Fe-N-C catalysts, where we applied the same potential-scan protocol (upper plot) to $Fe_{0.5}$-Ar and $Fe_{0.5}$-NH_3 in oxygen-saturated electrolyte. The electrode was first contacted by the SFC (corresponding time marked with * in the graph, t ~ 250 s) at open circuit potential (OCP). The applied electrochemical potential protocol is then 20 cyclic voltammograms (CVs) in the range 1.0 to 0.6 V vs. RHE at a scan rate of 100 $mV \cdot s^{-1}$, a potential range typically occurring during the ORR in fuel cell devices. Another chronoamperometry at 1.0 V was recorded for 200 s, before applying one CV at a low scan rate of 2 $mV \cdot s^{-1}$ from 1.0 V down to 0.0 V vs. RHE, and back up to 1.0 V vs. RHE to identify in more detail the potential-dependence of Fe dissolution.

The curves of Fe dissolution rate vs. time of both catalysts are nearly superimposed (from immersion to OCP hold, time 250 to 850 s on x-axis), with a peak value of Fe dissolution rate of ca 0.5 $ng_{Fe} \cdot cm^{-2} \cdot s^{-1}$, quickly decreasing (only ca 0.1 $ngFe \cdot cm^{-2} \cdot s^{-1}$ before starting the fast CVs). Therefore, both catalysts seem stable in alkaline medium. During the slow CV in alkaline electrolyte, there is no significant effect of the electrochemical potential in the negative-going branch of the scan, while reverting the scan direction from 0.0 V and upwards resulted in increased Fe dissolution rate for $Fe_{0.5}$-Ar but unmodified Fe dissolution rate for $Fe_{0.5}$-NH_3. These experiments were repeated multiple times, and showed reproducible trends.

The cumulative dissolved Fe content during these experiments was also obtained from the integral of the curves shown in the lower panels of Figure 6, while the total Fe content in each electrode was derived

from i) the fixed Fe-N-C catalyst loading value and the exact geometric area investigated by SFC-ICP-MS (verified each time by a microscope) and ii) the knowledge of the initial Fe content in each catalyst. The latter were measured by ICP-MS on the catalyst powders to be 1.45 wt% for $Fe_{0.5}$-Ar and 1.57 wt% for $Fe_{0.5}$-NH_3. The calculations conclude that only 5 to 10% relative Fe content is dissolved after 20 fast CVs and a slow scan, for both catalysts. This initial Fe dissolution is therefore restricted to a small fraction of Fe, and the lower panel of Figure 6 also show that the dissolution is stopped after the AST, while the ORR activity before/after AST is almost identical (Figures 3 and 5). All this indicates promising stability in AEMFC.

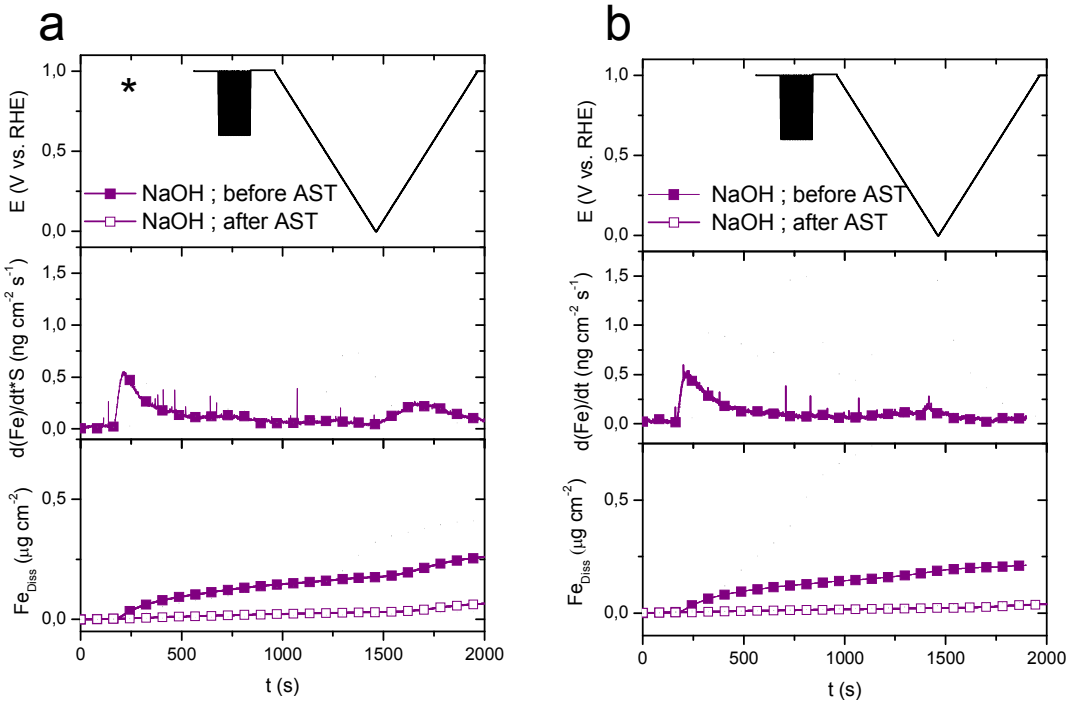

Figure 6. *Time-resolved potential (top) dissolution rates (middle) and totally dissolved amount (bottom) of iron from $Fe_{0.5}$-Ar (a) and $Fe_{0.5}$-NH_3 (b). The contact dissolution peak is marked with an asterisk in the upper panels. Dissolution rates after AST have been omitted for clarity in the middle panels since they are negligible. The experiments were conducted in 0.05 M NaOH.*

The demetallation of manganese was also investigated *in situ*, with SFC-ICP–MS measurements on α–Mn_2O_3 and other Mn-oxides (Figure 7). The figure shows that α–Mn_2O_3 is the most stable of the Mn-oxides at 0.6 V vs. RHE, a typical cathode potential for reaching high power density in AEMFC. Its low Mn leaching rate is primarily assigned to its lower BET area vs. that of the other Mn-oxides, and as a secondary factor, due to structural effect of the crystallographic phase. Since the surface specific activity of α–Mn_2O_3 for peroxide reduction is much higher than that of the other oxides, its low BET area is not detrimental and it is thus preferable to select α–Mn_2O_3 as a peroxide catalyst scavenger for combination with Fe-N-C in composite cathodes.

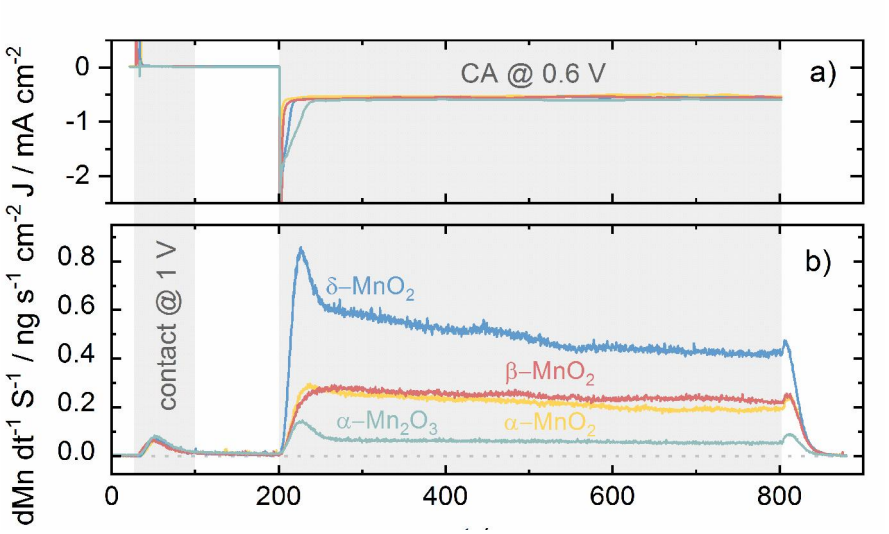

Figure 7. *Chronoamperometric (CA) curves recorded on all Mn-oxide catalysts over 10 min at 0.6 V_{RHE} in O_2 saturated 0.05 M NaOH (a) and Mn dissolution rate vs time (b).*

4. PERFORMANCE OF FE-N-C AND Mn_2O_3/FE-N-C CATHODES IN AEMFC

4.1 AEMFC PERFORMANCE WITH $Fe_{0.5}$-NH_3 CATHODE

Typical AEMFC polarization curve in O_2/H_2 obtained at 65°C on the MEA combining the $Fe_{0.5}$-NH_3 cathode and PtRu/C anode are shown in Figure 8. The peak power density was 1.4 W cm^{-2} reached at *ca* 0.4 V, while the initial activity at 0.9 V was *ca* 75 mA cm^{-2} (see inset). Below 0.2 V, the polarization curve shows a peculiar shape similar to a hook, typical for water management issues. Similar performance was obtained with $Fe_{0.5}$-NH_3 loadings of 1.5-2 mg cm^{-2} (see Table 1, further below) The ORR activity at 0.9 V at this moderate temperature and low catalyst loading (0.91 mg cm^{-2}) is extremely promising for replacing platinum, and peak power density already close to state-of-art obtained with Pt-based catalysts.

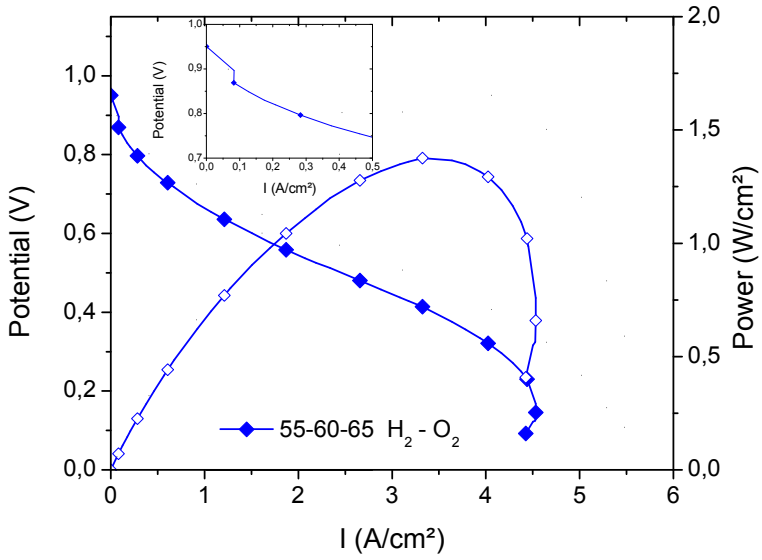

Figure 8. *H_2/O_2 AEMFC polarisation curves with $Fe_{0.5}$-NH_3 cathode (0.91 mg cm^{-2}). The anode was PtRu/C (Pt + Ru loading 0.6mg_{PGM} cm^{-2}). The curves were acquired at scan rate of 10 mV s^{-1}. The flow rate are 1 L min^{-1} on both sides. The cathode and anode dew points are 60°C and 55°C and cell temperature 65°C.*

4.2 AEMFC PERFORMANCE WITH Mn_2O_3/$Fe_{0.5}$-NH_3 CATHODE AND COMPARISON TO PLATINUM

The composite catalyst Mn_2O_3/$Fe_{0.5}$-NH_3 was tested in AEMFC, showing comparable initial activity (at 0.9 V) to platinum/C commercial catalyst and also to the $Fe_{0.5}$-NH_3 catalyst (Figure 9). At lower potential, the maximum current density reached with $Fe_{0.5}$-NH_3 cathode is ~ 2.5 A cm^{-2}, while for the composite catalyst is it ~2.7 A cm^{-2}, possibly due to an effect of the Mn-oxide. In RRDE setup, it was seen that the $Fe_{0.5}$-NH_3 catalyst has higher production of peroxide at low potential than the composite catalyst, which could reduce the current density at low cell voltage. In the composite catalyst, the presence of the Mn-oxide increases the conversion of the peroxide to water, possibly increasing the limiting current that is reached in operating fuel cell. Alternatively, modified hydrophilicity of the electrode with the addition of Mn-oxide could explain this result. The Pt/C cathode with high Pt loading of 0.4 mg_{Pt} cm^{-2} reaches, in the same conditions, circa 60% more current density at 0.6 V (black curve in Figure 9).

The beginning-of-life performance with the composite $Mn_2O_3/Fe_{0.5}$-NH_3 cathode is therefore promising, and longer durability test are planned to investigate its durability compared to the $Fe_{0.5}$-NH_3 cathode.

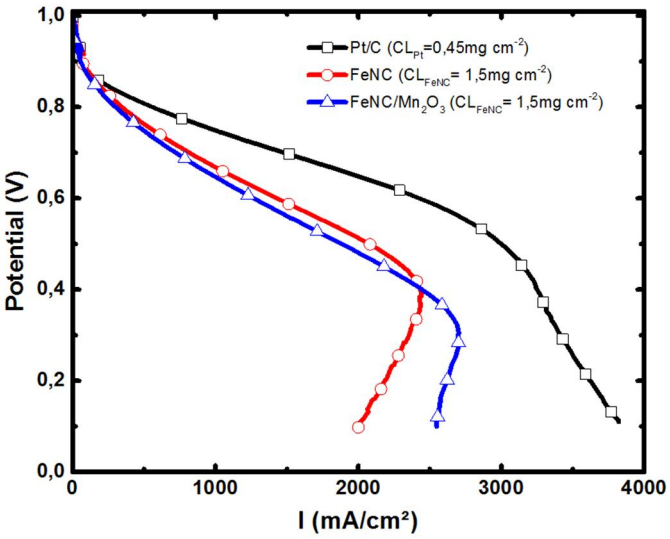

Figure 9. H_2/O_2 AEMFC polarisation curves for three different cathodes, and fixed anode and membrane. The curves were acquired at scan rate of 10 mV s^{-1}. The flow rate are 1 L min^{-1} on both sides. The cathode and anode dew points are 60°C and 55°C and cell temperature 65°C.

The Table 1 below summarizes the key performance results obtained for nine different MEAs tested in H_2/O_2 conditions, with PGM-free cathodes and different PtRu anode loadings.

Table 1. MEA compositions tested in AEMFC and key performance indicators. Cell temperature 65°C, optimized humidification of the gases. The AEI in electrodes was the same in all MEAs.

Cathode	AEM	Anode	Activity at 0.9 V / mA cm^{-2}	Peak Power Density / W cm^{-2}
Pt/C (0.45 mg_{PGM} cm^{-2})	AEM-1	PtRu/C (0.90 mg_{PGM} cm^{-2})	57	1.52
$Fe_{0.5}$-NH_3 (1.5 mg_{FeNC} cm^{-2})	AEM-1	PtRu/C (40%wt PGM) (0.9 mg_{PGM} cm^{-2})	66	1.05
$Fe_{0.5}$-NH_3/Mn_2O_3 (1.5 mg_{FeNC} cm^{-2})	AEM-1	PtRu/C (40%wt PGM) (0.9 mg_{PGM} cm^{-2})	53	0.99
$Fe_{0.5}$-NH_3 (1.0 mg_{FeNC} cm^{-2})	AEM-1	PtRu/C (40%wt PGM) (0.45 mg_{PGM} cm^{-2})	59	0.52
$Fe_{0.5}$-NH_3/Mn_2O_3 (1.5 mg_{FeNC} cm^{-2})	AEM-1	PtRu/C (40%wt PGM) (0.45 mg_{PGM} cm^{-2})	100	0.58
$Fe_{0.5}$-NH_3 (1.0 mg_{FeNC} cm^{-2})	AEM-1	PtRu/C (40%wt PGM) (0.11 mg_{PGM} cm^{-2})	29	0.35
$Fe_{0.5}$-NH_3 (1.0 mg_{FeNC} cm^{-2})	AEM-1	PtRu/CNT (5 wt% PGM) (0.095 mg_{PGM} cm^{-2})	55	0.23
$Fe_{0.5}$-NH_3 (1.5 mg_{FeNC} cm^{-2})	AEM-2	PtRu/C (40%wt PGM) (0.45 mg_{PGM} cm^{-2})	113	0.63
$Fe_{0.5}$-NH_3 (0.91 mg cm^{-2})	AEM-3	PtRu/C (40%wt PGM) (0.6 mg_{PGM} cm^{-2})	51	1.37

4.3 Performance and durability of $Fe_{0.5}$-NH_3 cathode in AEMFC with air feed

After determination of initial performance of Fe-$_{0.5}$-NH_3 cathode and composite Mn_2O_3/Fe-$_{0.5}$-NH_3 cathode in AEMFC fed with pure oxygen, further testing was performed with synthetic air, free of CO_2. Figure 10 shows air/H_2 polarization curves obtained at 65°C cell temperature, evidencing an activity of 20 mA cm^{-2} at 0.9 V, *ca* 20 % the value reached in pure oxygen, in line with the reduced concentration of O_2 in air (21 %). The polarization curve has a maximum current density of *ca* 2.4 A cm^{-2} and a peak power density of 0.7 W cm^{-2}, underlying the great performance of the $Fe_{0.5}$-NH_3 cathode in AEMFC fed with air.

The MEA durability was then determined applying 100 h chronopotentiometry at 600 mA cm^{-2} at a cell temperature of 65°C. Figure 11 shows a restricted decrease in the cell voltage from 0.69 V to 0.59 V over 100 h at 0.6 A·cm^{-2}, which is accompanied by a continuous increase in the high frequency resistance with time (not shown). At 0.85 V, the current density in the initial and final polarisation curves however only decreased by *ca* 30%, evidencing high stability of the Fe-based active sites. This strongly contrasts with the observations in PEMFC for the same catalyst and that evidenced a very fast decay.

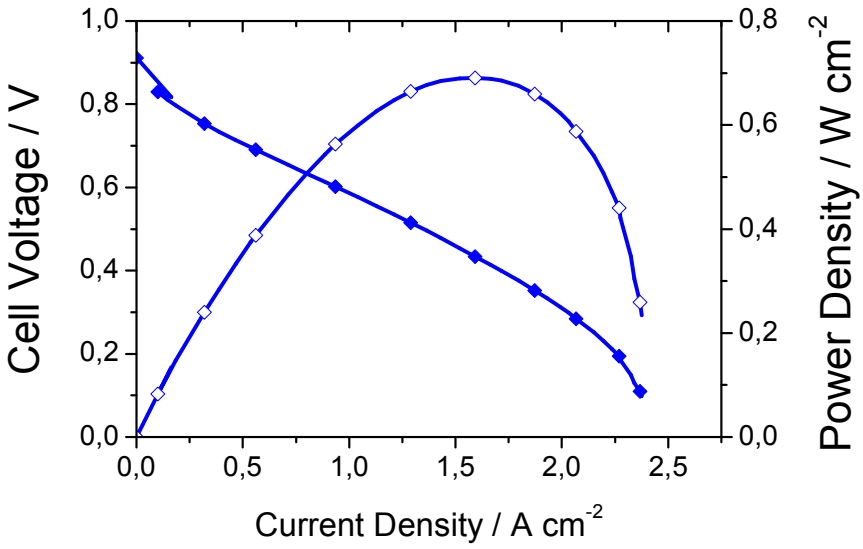

***Figure 10**. H_2/air Initial AEMFC polarisation curve. MEA comprising a $Fe_{0.5}$-NH_3 cathode (0.91 mg cm^{-2}), PtRu/C anode (PtRu loading 0.6 mg_{PGM} cm^{-2}). AEI/carbon ratio of 0.41 for PtRu/C anode catalyst, 0.2 for $Fe_{0.5}$-NH_3 cathode. Measured at a cell temperature of 65°C, dew points of 63°C and 58°C for cathode and anode respectively. The curves are measured at a scan rate of 10 mV s^{-1}.*

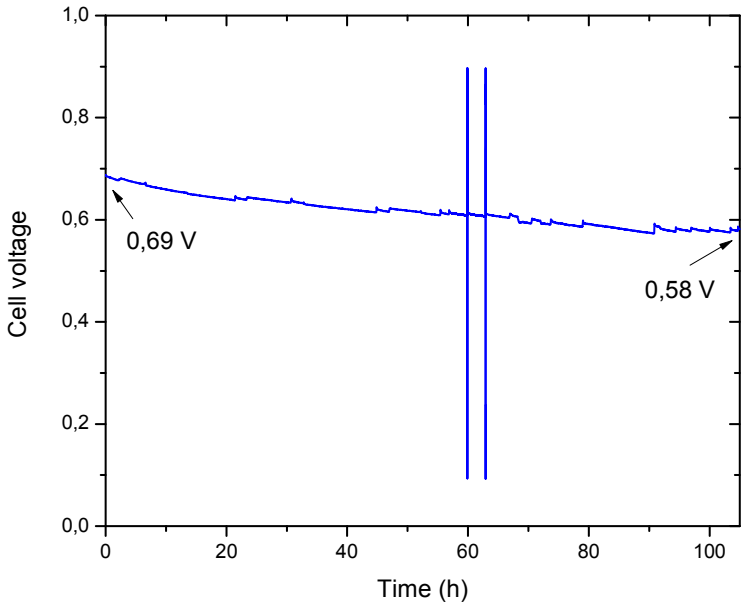

Figure 11. Durability test at constant current density of 0.6 A·cm^{-2} in H_2/air conditions. MEA comprising a $Fe_{0.5}$-NH_3 cathode (0.91 mg cm^{-2}), PtRu/C anode (PtRu loading 0.6 mg_{PGM} cm^{-2}). AEI/carbon ratio 0.41 for PtRu/C anode catalyst, 0.2 for $Fe_{0.5}$-NH_3 cathode. Measured at a cell temperature of 65°C, dew points of 63°C and 58°C for cathode and anode respectively. The curves are measured at a scan rate of 10 mV s^{-1}. The vertical lines result from the recording of polarisation curves during the galvanostatic test.

Conclusions

The $Fe_{0.5}$-NH_3 catalyst showed high activity in rotating disk electrode, with a mass-normalized activity of around 9 A g^{-1} at 0.9 V vs. RHE. This catalyst has been tested in H_2/O_2 AEMFC, which results in high peak power density of 1.4 W cm^{-2} and maximum current density of 4.7 A cm^{-2} at 65°C cell temperature. These results are above the previously best reported results for a non-PGM cathode catalyst in AEMFC.

In H_2/Air AEMFC at 65°C, the MEA with the $Fe_{0.5}$-NH_3 cathode reached a peak power density of 0.7 W cm^{-2} at 0.4 V and a maximum current density around 2.4 A cm^{-2}. Stability test at 600 mA cm^{-2} for 100 h showed a 100 mV decrease in the cell voltage, underlying the promising stability of the MEA. In addition, the polarization curves obtained before and after the stability test have been compared showing a small decrease in the ORR activity at 0.8 V (about -34 %), which underline the great stability of the $Fe_{0.5}$-NH_3 cathode catalyst.

REFERENCES

1. Pietro Giovanni Santori, Florian Speck, Jingkun Li, Andrea Zitolo, Qingying Jia, Sanjeev Mukerjee, Serhiy Cherevko, Frédéric Jaouen, Effect of pyrolysis atmosphere and electrolyte pH on the oxygen reduction activity, stability and spectroscopic signature of FeN_x moieties in Fe-N-C catalysts, J. Electrochem. Soc. 166 (2019) F3311-F3320.
2. Andrea Zitolo, Vincent Goellner, Vanessa Armel, Moulay-Tahar Sougrati, Tzonka Mineva, Lorenzo Stievano, Emiliano Fonda, Frédéric Jaouen, Identification of catalytic sites for oxygen reduction in iron- and nitrogen-doped graphene materials, Nature Mater. 14 (2015) 937-942.
3. Tzonka Mineva, Ivana Matanovic, Plamen Atanassov, Moulay-Tahar Sougrati, Lorenzo Stievano, Martin Clémancey, Amélie Kochem, Jean-Marc Latour, Frédéric Jaouen, Understanding active sites in pyrolyzed Fe-N-C catalysts for fuel cell cathodes by bridging density functional theory calculations and ^{57}Fe Mössbauer spectroscopy, ACS Catal. 9 (2019) 9359-9371.
4. T. J. Omasta et al., *J. Power Sources*, **375**, 205–213 (2018) https://doi.org/10.1016/j.jpowsour.2017.05.006.